

# Towards unification of quark and lepton flavors in $A_4$ modular invariance

Hiroshi Okada <sup>a\*</sup> and Morimitsu Tanimoto <sup>b†</sup>

<sup>a</sup>*Asia Pacific Center for Theoretical Physics (APCTP) - Headquarters San 31, Hyoja-dong,  
Nam-gu, Pohang 790-784, Korea*

<sup>b</sup>*Department of Physics, Niigata University, Niigata 950-2181, Japan*

## Abstract

We study quark and lepton mass matrices in the  $A_4$  modular invariance towards the unification of the quark and lepton flavors. We adopt modular forms of weights 2 and 6 for the quarks and charged leptons while we use modular forms of weight 4 for the neutrino mass matrix generated by the Weinberg operator. The modulus  $\tau$  is common in both quark and lepton mass matrices. We obtain the successful quark mass matrices, in which the down-type quark mass matrix is constructed by modular forms of weight 2, but the up-type quark mass matrix is constructed by modular forms of weight 6. Inputting observed masses and flavor mixing of quarks and leptons, model parameters are almost fixed as well as the value of modulus  $\tau$ . Supposing that the charged lepton mass matrix is constructed by modular forms of weight 2,  $\sin^2 \theta_{23}$  is predicted around 0.46–0.47 for the normal hierarchy of neutrino masses. The CP violating Dirac phase is also predicted as  $\delta_{CP}^\ell = 100^\circ\text{--}120^\circ$  or  $240^\circ\text{--}260^\circ$ , which is mainly originated from the modulus  $\tau$ . The effective neutrino mass of the  $0\nu\beta\beta$  decay is  $\langle m_{ee} \rangle = 4\text{--}18\text{meV}$  and the sum of neutrino masses is  $90\text{meV}$ . The inverted hierarchy of neutrino masses is excluded in our scheme of the  $A_4$  modular invariance. These predictions will be tested in the near future neutrino experiments.

---

<sup>\*</sup>E-mail address: hiroshi.okada@apctp.org

<sup>†</sup>E-mail address: tanimoto@muse.sc.niigata-u.ac.jp

# 1 Introduction

The standard model (SM) was well established by the discovery of the Higgs boson. However, the flavor theory of quarks and leptons is still unknown. In order to understand the origin of the flavor structure, many works have appeared by using the discrete groups for flavors. In the early models of quark masses and mixing angles, the  $S_3$  symmetry was used [1, 2]. It was also discussed to understand the large mixing angle [3] in the oscillation of atmospheric neutrinos [4]. For the last twenty years, the discrete symmetries of flavors have been developed, that is motivated by the precise observation of flavor mixing angles of leptons [5–13].

Many models have been proposed by using the non-Abelian discrete groups  $S_3$ ,  $A_4$ ,  $S_4$ ,  $A_5$  and other groups with larger orders to explain the large neutrino mixing angles. Among them, the  $A_4$  flavor model is attractive one because the  $A_4$  group is the minimal one including a triplet irreducible representation, which allows for a natural explanation of the existence of three families of leptons [14–20]. However, variety of models is so wide that it is difficult to obtain a clear evidence of the  $A_4$  flavor symmetry.

Recently, a new approach to the lepton flavor problem appeared based on the invariance under the modular group [21], where the model of the finite modular group  $\Gamma_3 \simeq A_4$  has been presented. This work inspired further studies of the modular invariance to the lepton flavor problem. It should be emphasized that there is a significant difference between the models based on the  $A_4$  modular symmetry and those based on the usual non-Abelian discrete  $A_4$  flavor symmetry. Yukawa couplings transform non-trivially under the modular group and are written in terms of modular forms which are holomorphic functions of a complex parameter, the modulus  $\tau$ .

The modular group includes  $S_3$ ,  $A_4$ ,  $S_4$ , and  $A_5$  as its finite subgroups [22]. Therefore, an interesting framework for the construction of flavor models has been put forward based on the  $\Gamma_3 \simeq A_4$  modular group [21], and further, based on  $\Gamma_2 \simeq S_3$  [23]. The proposed flavor models with modular symmetries  $\Gamma_4 \simeq S_4$  [24] and  $\Gamma_5 \simeq A_5$  [25] have also stimulated studies of flavor structures of quarks and leptons. Phenomenological discussions of the neutrino flavor mixing have been done based on  $A_4$  [26, 27],  $S_4$  [28] and  $A_5$  [29] modular groups, respectively. In particular, the comprehensive analysis of the  $A_4$  modular group has provided a distinct prediction of the neutrino mixing angles and the CP violating phase [27]. The  $A_4$  modular symmetry has been also applied to the  $SU(5)$  grand unified theory (GUT) of quarks and leptons [30], while the residual symmetry of the  $A_4$  modular symmetry has been investigated phenomenologically [31]. Furthermore, modular forms for  $\Delta(96)$  and  $\Delta(384)$  were constructed [32], and the extension of the traditional flavor group is discussed with modular symmetries [33]. The modular invariance has been also studied combining with the generalized CP symmetries for theories of flavors [34]. The quark mass matrix has been discussed in the  $S_3$  and  $A_4$  modular symmetries as well [35, 36]. Besides mass matrices of quarks and leptons, related topics have been discussed in the baryon number violation [35], the dark matter [37] and the modular symmetry anomaly [38].

In this work, we study both quarks and leptons in the  $A_4$  modular symmetry. If the flavor of quarks and leptons is originated from a same two-dimensional compact space, the quarks and leptons have same flavor symmetry and the same value of the modulus  $\tau$ . Therefore, it is challenging to reproduce observed hierarchical three Cabibbo-Kobayashi-Maskawa (CKM) mixing angles and the CP violating phase while observed large mixing angles are also reproduced in the lepton sector within the framework of the  $A_4$  modular invariance with the common  $\tau$ . This work provides a new aspect in order to discover the unification theory of the quark and lepton flavors. We have

already discussed the quark mass matrices in terms of  $A_4$  modular forms of weight 2. It has been found that quark mass matrices of  $A_4$  do not work unless Higgs sector is extended to the  $A_4$  triplet representation. In this paper, we propose to adopt modular forms of weight 6 in addition to modular ones of weight 2 for quarks with the Higgs sector of SM. We also use modular forms of weight 4 for the neutrino mass matrix generated by the Weinberg operator. By taking the common value of modulus  $\tau$ , we obtain the successful CKM mixing matrix and Pontecorvo-Maki-Nakagawa-Sakata (PMNS) matrix. Finally, we predict the CP violating Dirac phase of leptons, which is expected to be observed at T2K and NO $\nu$ A experiments [39, 40].

The paper is organized as follows. In section 2, we give a brief review on the modular symmetry and modular forms of weights 2, 4 and 6. In section 3, we present the model for quark mass matrices in the  $A_4$  modular symmetry. In section 4, we show numerical results for the CKM matrix. In section 5, we discuss the lepton mass matrices and present numerical results. Section 6 is devoted to a summary. In Appendix A, the tensor product of the  $A_4$  group is presented. In Appendix B, we show how to determine the coupling coefficients of quarks. In Appendix C, we present how to obtain Dirac  $CP$  phase, Majorana phases and effective mass of the  $0\nu\beta\beta$  decay.

## 2 Modular group and modular forms of weights 2, 4, 6

The modular group  $\bar{\Gamma}$  is the group of linear fractional transformation  $\gamma$  acting on the modulus  $\tau$ , belonging to the upper-half complex plane as:

$$\tau \longrightarrow \gamma\tau = \frac{a\tau + b}{c\tau + d}, \quad \text{where } a, b, c, d \in \mathbb{Z} \text{ and } ad - bc = 1, \quad \text{Im}[\tau] > 0, \quad (1)$$

which is isomorphic to  $PSL(2, \mathbb{Z}) = SL(2, \mathbb{Z})/\{I, -I\}$  transformation. This modular transformation is generated by  $S$  and  $T$ ,

$$S : \tau \longrightarrow -\frac{1}{\tau}, \quad T : \tau \longrightarrow \tau + 1, \quad (2)$$

which satisfy the following algebraic relations,

$$S^2 = \mathbb{I}, \quad (ST)^3 = \mathbb{I}. \quad (3)$$

We introduce the series of groups  $\Gamma(N)$  ( $N = 1, 2, 3, \dots$ ) defined by

$$\Gamma(N) = \left\{ \begin{pmatrix} a & b \\ c & d \end{pmatrix} \in SL(2, \mathbb{Z}), \quad \begin{pmatrix} a & b \\ c & d \end{pmatrix} = \begin{pmatrix} 1 & 0 \\ 0 & 1 \end{pmatrix} \pmod{N} \right\}. \quad (4)$$

For  $N = 2$ , we define  $\bar{\Gamma}(2) \equiv \Gamma(2)/\{I, -I\}$ . Since the element  $-I$  does not belong to  $\Gamma(N)$  for  $N > 2$ , we have  $\bar{\Gamma}(N) = \Gamma(N)$ , which are infinite normal subgroup of  $\bar{\Gamma}$ , called principal congruence subgroups. The quotient groups defined as  $\Gamma_N \equiv \bar{\Gamma}/\bar{\Gamma}(N)$  are finite modular groups. In this finite groups  $\Gamma_N$ ,  $T^N = \mathbb{I}$  is imposed. The groups  $\Gamma_N$  with  $N = 2, 3, 4, 5$  are isomorphic to  $S_3$ ,  $A_4$ ,  $S_4$  and  $A_5$ , respectively [22].

Modular forms of level  $N$  are holomorphic functions  $f(\tau)$  transforming under the action of  $\Gamma(N)$  as:

$$f(\gamma\tau) = (c\tau + d)^k f(\tau), \quad \gamma \in \Gamma(N), \quad (5)$$

where  $k$  is the so-called as the modular weight.

Superstring theory on the torus  $T^2$  or orbifold  $T^2/Z_N$  has the modular symmetry [41–46]. Its low energy effective field theory is described in terms of supergravity theory, and string-derived supergravity theory has also the modular symmetry. Under the modular transformation of Eq.(1), chiral superfields  $\phi^{(I)}$  transform as [47],

$$\phi^{(I)} \rightarrow (c\tau + d)^{-k_I} \rho^{(I)}(\gamma) \phi^{(I)}, \quad (6)$$

where  $-k_I$  is the modular weight and  $\rho^{(I)}(\gamma)$  denotes an unitary representation matrix of  $\gamma \in \Gamma(N)$ .

The kinetic terms of their scalar components are written by

$$\sum_I \frac{|\partial_\mu \phi^{(I)}|^2}{(-i\tau + i\bar{\tau})^{k_I}}, \quad (7)$$

which is invariant under the modular transformation. Here, the superfield and its scalar component are denoted by the same letter, and  $\bar{\tau} = \tau^*$  after taking the vacuum expectation value (VEV). Also, the superpotential should be invariant under the modular symmetry. That is, the superpotential should have vanishing modular weight in global supersymmetric models. In the following sections, we study global supersymmetric models, e.g. minimal supersymmetric standard model (MSSM). Thus, the superpotential has vanishing modular weight, which is realized by assigning relevant weights to superfields.

For  $\Gamma_3 \simeq A_4$ , the dimension of the linear space  $\mathcal{M}_k(\Gamma_3)$  of modular forms of weight  $k$  is  $k + 1$  [48–50], i.e., there are three linearly independent modular forms of the lowest non-trivial weight 2. These forms have been explicitly obtained [21] in terms of the Dedekind eta-function  $\eta(\tau)$ :

$$\eta(\tau) = q^{1/24} \prod_{n=1}^{\infty} (1 - q^n), \quad q = \exp(i2\pi\tau), \quad (8)$$

where  $\eta(\tau)$  is a so called modular form of weight 1/2. In what follows we will use the following basis of the  $A_4$  generators  $S$  and  $T$  in the triplet representation:

$$S = \frac{1}{3} \begin{pmatrix} -1 & 2 & 2 \\ 2 & -1 & 2 \\ 2 & 2 & -1 \end{pmatrix}, \quad T = \begin{pmatrix} 1 & 0 & 0 \\ 0 & \omega & 0 \\ 0 & 0 & \omega^2 \end{pmatrix}, \quad (9)$$

where  $\omega = \exp(i\frac{2}{3}\pi)$ . The modular forms of weight 2,  $\mathbf{Y}_3^{(2)} = (Y_1(\tau), Y_2(\tau), Y_3(\tau))^T$  transforming as a triplet of  $A_4$  can be written in terms of  $\eta(\tau)$  and its derivative [21]:

$$\begin{aligned} Y_1(\tau) &= \frac{i}{2\pi} \left( \frac{\eta'(\tau/3)}{\eta(\tau/3)} + \frac{\eta'((\tau+1)/3)}{\eta((\tau+1)/3)} + \frac{\eta'((\tau+2)/3)}{\eta((\tau+2)/3)} - \frac{27\eta'(3\tau)}{\eta(3\tau)} \right), \\ Y_2(\tau) &= \frac{-i}{\pi} \left( \frac{\eta'(\tau/3)}{\eta(\tau/3)} + \omega^2 \frac{\eta'((\tau+1)/3)}{\eta((\tau+1)/3)} + \omega \frac{\eta'((\tau+2)/3)}{\eta((\tau+2)/3)} \right), \\ Y_3(\tau) &= \frac{-i}{\pi} \left( \frac{\eta'(\tau/3)}{\eta(\tau/3)} + \omega \frac{\eta'((\tau+1)/3)}{\eta((\tau+1)/3)} + \omega^2 \frac{\eta'((\tau+2)/3)}{\eta((\tau+2)/3)} \right). \end{aligned} \quad (10)$$

The overall coefficient in Eq. (10) is one possible choice. It cannot be uniquely determined. The triplet modular forms of weight 2 have the following  $q$ -expansions:

$$\mathbf{Y}_3^{(2)} = \begin{pmatrix} Y_1(\tau) \\ Y_2(\tau) \\ Y_3(\tau) \end{pmatrix} = \begin{pmatrix} 1 + 12q + 36q^2 + 12q^3 + \dots \\ -6q^{1/3}(1 + 7q + 8q^2 + \dots) \\ -18q^{2/3}(1 + 2q + 5q^2 + \dots) \end{pmatrix}. \quad (11)$$

They satisfy also the constraint [21]:

$$(Y_2(\tau))^2 + 2Y_1(\tau)Y_3(\tau) = 0. \quad (12)$$

The modular forms of the higher weight,  $k$ , can be obtained by the  $A_4$  tensor products of the modular forms with weight 2,  $\mathbf{Y}_3^{(2)}$ , as given in Appendix A. For  $k = 4$ , there are five modular forms by the tensor product of  $\mathbf{3} \otimes \mathbf{3}$  as:

$$\begin{aligned} \mathbf{Y}_1^{(4)} &= Y_1^2 + 2Y_2Y_3, \quad \mathbf{Y}_{1'}^{(4)} = Y_3^2 + 2Y_1Y_2, \quad \mathbf{Y}_{1''}^{(4)} = Y_2^2 + 2Y_1Y_3 = 0, \\ \mathbf{Y}_3^{(4)} &= \begin{pmatrix} Y_1^2 - Y_2Y_3 \\ Y_3^2 - Y_1Y_2 \\ Y_2^2 - Y_1Y_3 \end{pmatrix}, \end{aligned} \quad (13)$$

where  $\mathbf{Y}_{1''}^{(4)}$  vanishes due to the constraint of Eq. (12). For  $k = 6$ , there are seven modular forms by the tensor products of  $A_4$  as:

$$\begin{aligned} \mathbf{Y}_1^{(6)} &= Y_1^3 + Y_2^3 + Y_3^3 - 3Y_1Y_2Y_3, \\ \mathbf{Y}_3^{(6)} &\equiv \begin{pmatrix} Y_1^{(6)} \\ Y_2^{(6)} \\ Y_3^{(6)} \end{pmatrix} = \begin{pmatrix} Y_1^3 + 2Y_1Y_2Y_3 \\ Y_1^2Y_2 + 2Y_2^2Y_3 \\ Y_1^2Y_3 + 2Y_3^2Y_2 \end{pmatrix}, \quad \mathbf{Y}_{3'}^{(6)} \equiv \begin{pmatrix} Y_1'^{(6)} \\ Y_2'^{(6)} \\ Y_3'^{(6)} \end{pmatrix} = \begin{pmatrix} Y_3^3 + 2Y_1Y_2Y_3 \\ Y_3^2Y_1 + 2Y_1^2Y_2 \\ Y_3^2Y_2 + 2Y_2^2Y_1 \end{pmatrix}. \end{aligned} \quad (14)$$

By using these modular forms of weights 2, 4, 6, we discuss quark and lepton mass matrices.

### 3 Quark mass matrices in the $A_4$ modular invariance

Let us consider a  $A_4$  modular invariant flavor model for quarks. There are freedoms for the assignments of irreducible representations and modular weights to quarks and Higgs doublets.

The simplest one is to assign the triplet of the  $A_4$  group to three left-handed quarks, but three different singlets ( $\mathbf{1}, \mathbf{1}'', \mathbf{1}'$ ) of  $A_4$  to the three right-handed quarks,  $(u^c, c^c, t^c)$  and  $(d^c, s^c, b^c)$ , respectively, where the sum of weights of the left-handed and the right-handed quarks is  $-2$ .

Then, there appear three independent couplings in the superpotential of the up-type and down-type quark sectors, respectively, as follows:

$$w_u = \alpha_u u^c H_u \mathbf{Y}_3^{(2)} Q + \beta_u c^c H_u \mathbf{Y}_3^{(2)} Q + \gamma_u t^c H_u \mathbf{Y}_3^{(2)} Q, \quad (15)$$

$$w_d = \alpha_d d^c H_d \mathbf{Y}_3^{(2)} Q + \beta_d s^c H_d \mathbf{Y}_3^{(2)} Q + \gamma_d b^c H_d \mathbf{Y}_3^{(2)} Q , \quad (16)$$

where  $Q$  is the left-handed  $A_4$  triplet quarks, and  $H_q$  is the Higgs doublets. The parameters  $\alpha_q$ ,  $\beta_q$ ,  $\gamma_q$  ( $q = u, d$ ) are constant coefficients. Assign the left-handed  $A_4$  triplet  $Q$  to  $(u_L, c_L, t_L)$  and  $(d_L, s_L, b_L)$ . By using the decomposition of the  $A_4$  tensor product in Appendix A, the superpotentials in Eqs.(15) and (16) give the mass matrix of quarks, which is written in terms of modular forms of weight 2:

$$M_q = v_q \begin{pmatrix} \alpha_q & 0 & 0 \\ 0 & \beta_q & 0 \\ 0 & 0 & \gamma_q \end{pmatrix} \begin{pmatrix} Y_1 & Y_3 & Y_2 \\ Y_2 & Y_1 & Y_3 \\ Y_3 & Y_2 & Y_1 \end{pmatrix}_{RL} , \quad (q = u, d) , \quad (17)$$

where  $\tau$  of the modular forms  $Y_i(\tau)$  is omitted. The coefficient  $v_q$  is the VEV of the Higgs field  $H_q$ . Unknown couplings  $\alpha_q$ ,  $\beta_q$ ,  $\gamma_q$  can be adjusted to the observed quark masses. The remained parameter is only the modulus,  $\tau$ . The numerical study of the quark mass matrix in Eq.(17) is rather easy. However, it is impossible to reproduce observed hierarchical three CKM mixing angles by fixing one complex parameter  $\tau$ .

	$Q$	$(q_1^c, q_2^c, q_3^c)$	$H_q$	$\mathbf{Y}_3^{(6)}, \mathbf{Y}_{3'}^{(6)}$
$SU(2)$	<b>2</b>	<b>1</b>	<b>2</b>	<b>1</b>
$A_4$	<b>3</b>	<b>(1, 1'', 1')</b>	<b>1</b>	<b>3, 3'</b>
$-k_I$	-2	<b>(-4, -4, -4)</b>	0	$k = 6$

Table 1: Assignments of representations and weights  $-k_I$  for MSSM fields and modular forms.

In order to present realistic quark mass matrices, we use modular forms of weight 6 as well as modular forms of weight 2. Since there are two triplets of  $A_4$  for weight 6 as seen in Eq.(14), the quark mass matrix is given by the linear combination of two matrices, where assignments of representations and weights for MSSM fields are given in Table 1:

$$M_q = v_q \begin{pmatrix} \alpha_q & 0 & 0 \\ 0 & \beta_q & 0 \\ 0 & 0 & \gamma_q \end{pmatrix} \left[ \begin{pmatrix} Y_1^{(6)} & Y_3^{(6)} & Y_2^{(6)} \\ Y_2^{(6)} & Y_1^{(6)} & Y_3^{(6)} \\ Y_3^{(6)} & Y_2^{(6)} & Y_1^{(6)} \end{pmatrix} + g_q \begin{pmatrix} Y_1'^{(6)} & Y_3'^{(6)} & Y_2'^{(6)} \\ Y_2'^{(6)} & Y_1'^{(6)} & Y_3'^{(6)} \\ Y_3'^{(6)} & Y_2'^{(6)} & Y_1'^{(6)} \end{pmatrix} \right]_{RL} , \quad (q = u \text{ or } d) , \quad (18)$$

where  $Y_i^{(6)}$  and  $Y_i'^{(6)}$  are given in Eq.(14). Parameters  $\alpha_q$ ,  $\beta_q$ ,  $\gamma_q$  are real, on the other hand,  $g_q$  is a complex parameter. Due to the new parameter  $g_q$ , the quark mass matrix could be consistent with the CKM observations.

Let us consider three cases of mass matrices by using modular forms of weights 2 and 6.

**Model-I : down-type quark mass matrix with  $\mathbf{Y}_3^{(2)}$  and up-type one with  $\mathbf{Y}_3^{(6)}$  and  $\mathbf{Y}_{3'}^{(6)}$**

$$M_d = v_d \begin{pmatrix} \alpha_d & 0 & 0 \\ 0 & \beta_d & 0 \\ 0 & 0 & \gamma_d \end{pmatrix} \begin{pmatrix} Y_1 & Y_3 & Y_2 \\ Y_2 & Y_1 & Y_3 \\ Y_3 & Y_2 & Y_1 \end{pmatrix}_{RL},$$

$$M_u = v_u \begin{pmatrix} \alpha_u & 0 & 0 \\ 0 & \beta_u & 0 \\ 0 & 0 & \gamma_u \end{pmatrix} \left[ \begin{pmatrix} Y_1^{(6)} & Y_3^{(6)} & Y_2^{(6)} \\ Y_2^{(6)} & Y_1^{(6)} & Y_3^{(6)} \\ Y_3^{(6)} & Y_2^{(6)} & Y_1^{(6)} \end{pmatrix} + g_u \begin{pmatrix} Y_1'^{(6)} & Y_3'^{(6)} & Y_2'^{(6)} \\ Y_2'^{(6)} & Y_1'^{(6)} & Y_3'^{(6)} \\ Y_3'^{(6)} & Y_2'^{(6)} & Y_1'^{(6)} \end{pmatrix} \right]_{RL}, \quad (19)$$

where assignments of representations and weights for MSSM fields are given in Table 2.

	$Q$	$(d^c, s^c, b^c)$	$(u^c, c^c, t^c)$	$H_{u,d}$	$\mathbf{Y}_3^{(2)}$	$\mathbf{Y}_3^{(6)}, \mathbf{Y}_{3'}^{(6)}$
$SU(2)$	<b>2</b>	<b>1</b>	<b>1</b>	<b>2</b>	<b>1</b>	<b>1</b>
$A_4$	<b>3</b>	$(\mathbf{1}, \mathbf{1}'', \mathbf{1}')$	$(\mathbf{1}, \mathbf{1}'', \mathbf{1}')$	<b>1</b>	<b>3</b>	<b>3, 3'</b>
$-k_I$	-2	(0, 0, 0)	(-4, -4, -4)	0	$k = 2$	$k = 6$

Table 2: Assignments of representations and weights  $-k_I$  for MSSM fields and modular forms of weight 2 and 6 in model-I.

**Model-II : down-type quark mass matrix with  $\mathbf{Y}_3^{(6)}$  and  $\mathbf{Y}_{3'}^{(6)}$  and up-type one with  $\mathbf{Y}_3^{(2)}$**

$$M_d = v_d \begin{pmatrix} \alpha_d & 0 & 0 \\ 0 & \beta_d & 0 \\ 0 & 0 & \gamma_d \end{pmatrix} \left[ \begin{pmatrix} Y_1^{(6)} & Y_3^{(6)} & Y_2^{(6)} \\ Y_2^{(6)} & Y_1^{(6)} & Y_3^{(6)} \\ Y_3^{(6)} & Y_2^{(6)} & Y_1^{(6)} \end{pmatrix} + g_d \begin{pmatrix} Y_1'^{(6)} & Y_3'^{(6)} & Y_2'^{(6)} \\ Y_2'^{(6)} & Y_1'^{(6)} & Y_3'^{(6)} \\ Y_3'^{(6)} & Y_2'^{(6)} & Y_1'^{(6)} \end{pmatrix} \right]_{RL},$$

$$M_u = v_u \begin{pmatrix} \alpha_u & 0 & 0 \\ 0 & \beta_u & 0 \\ 0 & 0 & \gamma_u \end{pmatrix} \begin{pmatrix} Y_1 & Y_3 & Y_2 \\ Y_2 & Y_1 & Y_3 \\ Y_3 & Y_2 & Y_1 \end{pmatrix}_{RL}, \quad (20)$$

where assignments of representations and weights for MSSM fields are given in Table 3.

	$Q$	$(d^c, s^c, b^c)$	$(u^c, c^c, t^c)$	$H_{u,d}$	$\mathbf{Y}_3^{(2)}$	$\mathbf{Y}_3^{(6)}, \mathbf{Y}_{3'}^{(6)}$
$SU(2)$	<b>2</b>	<b>1</b>	<b>1</b>	<b>2</b>	<b>1</b>	<b>1</b>
$A_4$	<b>3</b>	$(\mathbf{1}, \mathbf{1}'', \mathbf{1}')$	$(\mathbf{1}, \mathbf{1}'', \mathbf{1}')$	<b>1</b>	<b>3</b>	<b>3, 3'</b>
$-k_I$	-2	(-4, -4, -4)	(0, 0, 0)	0	$k = 2$	$k = 6$

Table 3: Assignments of representations and weights  $-k_I$  for MSSM fields and modular forms of weight 2 and 6 in model-II.

**Model-III : both down-type quark mass matrix and up-type one with  $Y_3^{(6)}$  and  $Y_{3'}^{(6)}$**

$$M_d = v_d \begin{pmatrix} \alpha_d & 0 & 0 \\ 0 & \beta_d & 0 \\ 0 & 0 & \gamma_d \end{pmatrix} \left[ \begin{pmatrix} Y_1^{(6)} & Y_3^{(6)} & Y_2^{(6)} \\ Y_2^{(6)} & Y_1^{(6)} & Y_3^{(6)} \\ Y_3^{(6)} & Y_2^{(6)} & Y_1^{(6)} \end{pmatrix} + g_d \begin{pmatrix} Y_1'^{(6)} & Y_3'^{(6)} & Y_2'^{(6)} \\ Y_2'^{(6)} & Y_1'^{(6)} & Y_3'^{(6)} \\ Y_3'^{(6)} & Y_2'^{(6)} & Y_1'^{(6)} \end{pmatrix} \right]_{RL},$$

$$M_u = v_u \begin{pmatrix} \alpha_u & 0 & 0 \\ 0 & \beta_u & 0 \\ 0 & 0 & \gamma_u \end{pmatrix} \left[ \begin{pmatrix} Y_1^{(6)} & Y_3^{(6)} & Y_2^{(6)} \\ Y_2^{(6)} & Y_1^{(6)} & Y_3^{(6)} \\ Y_3^{(6)} & Y_2^{(6)} & Y_1^{(6)} \end{pmatrix} + g_u \begin{pmatrix} Y_1'^{(6)} & Y_3'^{(6)} & Y_2'^{(6)} \\ Y_2'^{(6)} & Y_1'^{(6)} & Y_3'^{(6)} \\ Y_3'^{(6)} & Y_2'^{(6)} & Y_1'^{(6)} \end{pmatrix} \right]_{RL}, \quad (21)$$

where assignments of representations and weights for MSSM fields are given in Table 4. We discuss numerical results of these three models in the next section.

	$Q$	$(d^c, s^c, b^c)$	$(u^c, c^c, t^c)$	$H_{u,d}$	$Y_3^{(6)}, Y_{3'}^{(6)}$
$SU(2)$	<b>2</b>	<b>1</b>	<b>1</b>	<b>2</b>	<b>1</b>
$A_4$	<b>3</b>	$(1, 1'', 1')$	$(1, 1'', 1')$	<b>1</b>	<b>3, 3'</b>
$-k_I$	-2	$(-4, -4, -4)$	$(-4, -4, -4)$	0	$k = 6$

Table 4: Assignments of representations and weights  $-k_I$  for MSSM fields and modular forms of weight 6 in model-III.

## 4 Numerical results of CKM mixing

In order to obtain the left-handed flavor mixing, we calculate  $M_d^\dagger M_d$  and  $M_u^\dagger M_u$  for model-I, model-II and model-III, respectively. At first, we take a random point of  $\tau$  and  $g_q$  which are scanned in the complex plane by generating random numbers. The scanned ranges of  $\text{Im}[\tau]$  is  $[0.5, 10]$ , in which the lower-cut 0.5 comes from the accuracy of calculating modular forms, and the upper-cut 10 is enough large for estimating  $Y_i$  in practice. On the other hand,  $\text{Re}[\tau]$  is scanned in the fundamental region of  $[-3/2, 3/2]$  in Eq.(10) because the modular forms  $Y_i$  is given in terms of  $\eta(\tau/3)$ . We also scan in  $|g_u| \in [0, 2000]$  and  $|g_d| \in [0, 2000]$  while these phases are scanned in  $[-\pi, \pi]$ .

Then, parameters  $\alpha_q, \beta_q, \gamma_q$  ( $q = u, d$ ) are determined by computing forms  $C_i^q (i = 1-3)$  in Appendix B after inputting six quark masses (see Appendix B).

Finally, we calculate three CKM mixing angles in terms of the model parameters  $\tau, g_q$ , while keeping the parameter sets allowed by the experimental data of the CKM mixing angles. We continue this procedure to obtain enough points for plotting allowed region.

We input quark masses in order to constrain model parameters. Since the modulus  $\tau$  obtains the expectation value by the breaking of the modular invariance at the high mass scale, the quark masses are put at the GUT scale. The observed masses and CKM parameters run to the GUT scale by the renormalization group equations (RGEs). In our work, we adopt numerical values of Yukawa couplings of quarks at the GUT scale  $2 \times 10^{16}$  GeV with  $\tan \beta = 5$  in the framework of the minimal SUSY breaking scenarios [51, 52]:

$$y_d = (4.81 \pm 1.06) \times 10^{-6}, \quad y_s = (9.52 \pm 1.03) \times 10^{-5}, \quad y_b = (6.95 \pm 0.175) \times 10^{-3},$$

$$y_u = (2.92 \pm 1.81) \times 10^{-6}, \quad y_c = (1.43 \pm 0.100) \times 10^{-3}, \quad y_t = 0.534 \pm 0.0341, \quad (22)$$



which give quark masses as  $m_q = y_q v_H$  with  $v_H = 174$  GeV. We also use the following CKM mixing angles to focus on parameter regions consistent with the experimental data at the GUT scale  $2 \times 10^{16}$  GeV, where  $\tan \beta = 5$  is taken [51, 52]:

$$\theta_{12} = 13.027^\circ \pm 0.0814^\circ, \quad \theta_{23} = 2.054^\circ \pm 0.384^\circ, \quad \theta_{13} = 0.1802^\circ \pm 0.0281^\circ. \quad (23)$$

Here  $\theta_{ij}$  is given in the PDG notation of the CKM matrix  $V_{\text{CKM}}$  [53]. The error widths in Eqs.(22) and (23) represent  $1\sigma$  interval. In our numerical calculation, we take  $2\sigma$  interval for quark masses.

In the model-I, we have four real parameters, that is, free complex parameters  $\tau$  and  $g_u$  after inputting six quark masses. By constraining these parameters by three CKM mixing angles in Eq.(23) with  $3\sigma$  interval, we can predict the CP violating phase  $\delta_{CP}$ , which is given in the PDG notation [53]. We show the predicted  $\delta_{CP}$  versus the CKM element  $|V_{ub}|$  in Fig.1, in which  $\delta_{CP}$  should be compared with the observed one at the GUT scale  $2 \times 10^{16}$  GeV with  $\tan \beta = 5$  [51, 52]:

$$\delta_{CP} = 69.21^\circ \pm 6.19^\circ. \quad (24)$$

The predicted region is symmetric about the horizontal line of  $180^\circ$ . Some points are consistent with the experimental value of  $\delta_{CP}$  with  $3\sigma$  interval. They are rather lower value  $50^\circ$ – $55^\circ$ . However, we should take into account that the input parameters of Yukawa couplings in Eq.(22) are specific ones at  $\tan \beta = 5$ . We have checked that the predicted  $\delta_{CP}$  increases up to 10% according to decrease of  $\tan \beta$  towards 1. Numerical results of Yukawa couplings at the GUT scale also depend on the SUSY breaking scenario and its scale. Moreover, we have found that the predicted  $\delta_{CP}$  is expanded to  $\pm 10^\circ$  if  $3\sigma$  error-bar is taken for the input masses of Eq.(22) although input of masses with  $2\sigma$  interval are taken in Fig.1. Therefore, the predicted  $\delta_{CP}$  could be close to the central value of Eq.(24) if the input quark masses are modified relevantly. In conclusion, our predicted CP violating phase of model-I is completely consistent with the observed one.

We also show the allowed region of CKM elements  $|V_{cb}|$  and  $|V_{ub}|$  in Fig.2, where green (blue) points denote allowed ones with (without) constraint of observed  $\delta_{CP}$ . The magnitude of  $V_{cb}$  is predicted to be larger than the central value while calculated  $|V_{ub}|$  is close to the lower bound of the experimental data under the constraint of the observed  $\delta_{CP}$ . Those predictions are also relaxed if the input quark masses are modified relevantly.

In the model-II, we have also four real parameters, that is, free complex parameters  $\tau$  and  $g_d$  after inputting six quark masses. However, there is no allowed points consistent with three CKM mixing angles. The Cabibbo mixing angle and  $|V_{cb}|$  are easily reproduced by choosing relevant values for our parameters, but  $|V_{ub}|$  is unavoidably around the magnitude of  $V_{cb}$ .

Finally, we present the numerical result of model-III, where we have three complex parameters,  $\tau$ ,  $g_d$  and  $g_u$  after inputting six quark masses. That is, there are two additional real parameters compared with model-I and model-II. These additional parameters are available to reproduce the observed CKM elements. We show  $\delta_{CP}$  versus  $|V_{ub}|$  by constraining parameters with three CKM mixing angles of Eq.(23) in Fig.3. The predicted  $\delta_{CP}$  covers  $0$ – $2\pi$  and symmetric about the horizontal line of  $180^\circ$ . Thus, model-III allows any value for  $\delta_{CP}$ . Model parameters are restricted by imposing the observed CP violating phase as seen in Table 5.

We also show the allowed region of  $|V_{cb}|$  and  $|V_{ub}|$  in Fig.4, where green (blue) points denote allowed ones with (without) constraint of observed  $\delta_{CP}$ . The magnitude of  $V_{ub}$  is preferred to be smaller than the central value while calculated  $|V_{cb}|$  covers all range of the experimental data.

In Table 5, we summarize parameter ranges consistent with observed CKM mixing angles and the CP violating phase for both model-I and model-III. It is noticed that the imaginary part of  $g_q$

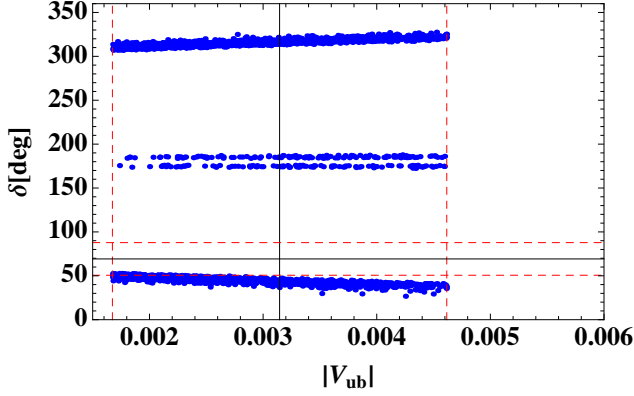


Figure 1: Predicted  $\delta_{CP}$  versus  $|V_{ub}|$ , where black lines denote observed central values of  $|V_{ub}|$  and  $\delta_{CP}$ , and red dashed-lines denote their upper-bounds and lower-bounds of  $3\sigma$  interval in model-I.

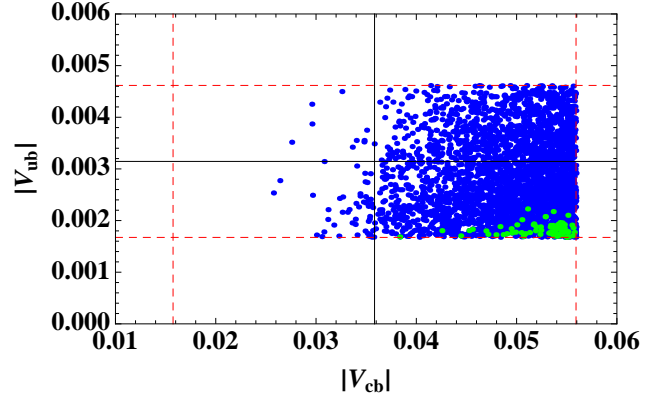


Figure 2: Allowed region on  $|V_{cb}|$ - $|V_{ub}|$  plane in model-I. Notation of black and red lines are same ones in Fig.1. Blue (green) points denote allowed ones without (with) constraint of observed  $\delta_{CP}$ .

is inevitable to reproduce the observed  $\delta_{CP}$  in addition to  $\text{Re}[\tau]$ , which provides imaginary parts in  $q$ ,  $q^{1/3}$  and  $q^{2/3}$  as seen in Eq.(11).

In Table 6, we show typical parameter sets and calculated CKM parameters in model-I and model-III, respectively. Ratios of  $\alpha_q/\gamma_q$  and  $\beta_q/\gamma_q$  ( $q = u, d$ ) in Table 6 correspond to the observed quark mass hierarchy.

	Model I	Model III
$\text{Re}[\tau]$	$\pm(0.957-1.045)$	$\pm(0.108-1.496)$
$\text{Im}[\tau]$	$0.957-1.045$	$1.206-1.594$
$\text{Re}[g_u]$	$-(0.140-0.149)$	$\pm(0.001-0.083)$
$\text{Im}[g_u]$	$0.198-0.210$	$\pm(0.001-0.136)$
$\text{Re}[g_d]$	—	$\pm(162-1459)$
$\text{Im}[g_d]$	—	$\pm(0.1-996)$

Table 5: Parameter ranges consistent with the observed CKM mixing angles and CP violating phase  $\delta_{CP}$  for model-I and model-III, respectively.

We also present the mixing matrices of down-type quarks and up-type quarks for two samples in order to investigate the flavor structure of each quark mass matrix. For the sample of model-I in Table 6, we obtain

$$|V_d| = \begin{pmatrix} 0.5537 & 0.6135 & 0.5631 \\ 0.8110 & 0.2439 & 0.5317 \\ 0.1889 & 0.7511 & 0.6326 \end{pmatrix}, \quad |V_u| = \begin{pmatrix} 0.4857 & 0.6859 & 0.5419 \\ 0.8198 & 0.2382 & 0.5208 \\ 0.3034 & 0.6876 & 0.6596 \end{pmatrix}, \quad (25)$$

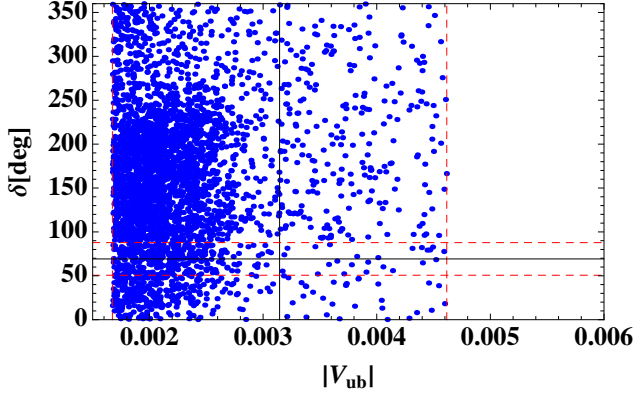


Figure 3: Predicted  $\delta_{CP}$  versus  $|V_{ub}|$ , where black lines denote observed central values of  $|V_{ub}|$  and  $\delta_{CP}$ , and red dashed-lines denote their upper-bounds and lower-bounds of  $3\sigma$  interval in model-III.

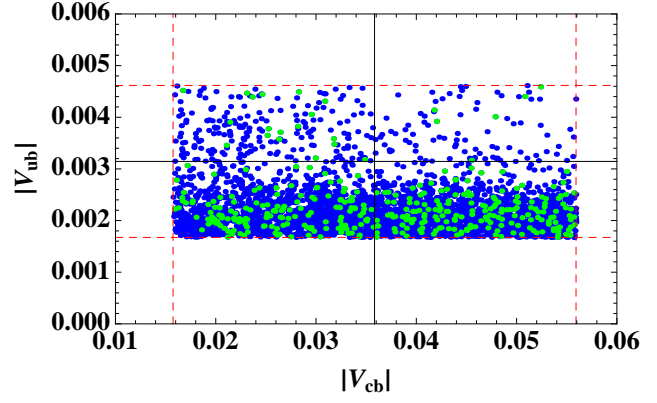


Figure 4: Allowed region on  $|V_{cb}|$ - $|V_{ub}|$  plane in model-III. Notation of black and red lines are same ones in Fig.3. Blue (green) points denote allowed ones without (with) constraint of observed  $\delta_{CP}$ .

where  $V_{CKM} = V_u^\dagger V_d$ . It is noticed that the flavor structure of quark mass matrices is anarchy. We have checked that the quark mass matrices are anarchy for all parameter sets of model-I. The observed CKM matrix is realized by the relevant cancellation between the down-type and up-type quark sectors.

For the sample of model-III in Table 6, we have

$$|V_d| = \begin{pmatrix} 0.0184 & 0.9737 & 0.2271 \\ 0.9964 & 0.0275 & 0.0804 \\ 0.0829 & 0.2262 & 0.9705 \end{pmatrix}, \quad |V_u| = \begin{pmatrix} 0.2175 & 0.9514 & 0.2179 \\ 0.9756 & 0.2062 & 0.0756 \\ 0.0302 & 0.2287 & 0.9730 \end{pmatrix}. \quad (26)$$

After exchanging rows or columns between 1st and 2nd ones, those are typical hierarchical mixing matrices. This exchange corresponds to  $(u_L, c_L, t_L) \rightarrow (c_L, u_L, t_L)$  or  $(d_L, s_L, b_L) \rightarrow (s_L, d_L, b_L)$  for the assignment of the  $A_4$  triplet. It is noted that the quark mass matrices are hierarchical for other all parameter sets of model-III.

In conclusion, our quark mass matrices with the  $A_4$  modular symmetry (model-I and model-III) can successfully reproduce the CKM mixing matrix completely with observed quark masses. This successful result encourages us to investigate the lepton sector in the same framework. We discuss the lepton mass matrices with the  $A_4$  modular symmetry in the next section.

## 5 Lepton mass matrix in the $A_4$ modular invariance

### 5.1 Lepton mass matrix

The modular  $A_4$  invariance also gives the lepton mass matrix in terms of the modulus  $\tau$  which is common both quarks and leptons if flavors of quarks and leptons are originated from a same two-dimensional compact space. The  $A_4$  representation and weight are assigned for lepton fields relevantly as seen in Table 7, where the left-handed lepton doublets compose a  $A_4$  triplet and the right-handed charged leptons are  $A_4$  singlets. Weights of leptons are assigned like as the quark ones in Table 7.

	Model-I	Model-III
$\tau$	$1.011 + 1.034 i$	$-1.130 + 1.552 i$
$g_u$	$-0.141 - 0.207 i$	$-0.026 + 0.077 i$
$g_d$	—	$1334 + 9.7 i$
$\alpha_u/\gamma_u$	$2.151 \times 10^2$	$3.408 \times 10^2$
$\beta_u/\gamma_u$	$7.602 \times 10^4$	$1.398 \times 10^5$
$\alpha_d/\gamma_d$	4.218	$3.615 \times 10^{-2}$
$\beta_d/\gamma_d$	$2.443 \times 10^2$	$7.253 \times 10$
$ V_{us} $	0.2252	0.2282
$ V_{cb} $	0.0444	0.0357
$ V_{ub} $	0.0017	0.0019
$\delta_{CP}$	$51.4^\circ$	$79.0^\circ$

Table 6: Numerical values of parameters and output of CKM parameters at the sample points for model-I and model-III, respectively.

	$L$	$(e^c, \mu^c, \tau^c)$	$H_u$	$H_d$	$\mathbf{Y}_r^{(2)}, \mathbf{Y}_r^{(4)}$
$SU(2)$	<b>2</b>	<b>1</b>	<b>2</b>	<b>2</b>	<b>1</b>
$A_4$	<b>3</b>	<b>(1, 1'', 1')</b>	<b>1</b>	<b>1</b>	<b>3, {3, 1, 1'}</b>
$-k_I$	-2	(0, 0, 0) or (-4, -4, -4)	0	0	2, 4

Table 7: Assignments of representations and weights  $-k_I$  for MSSM fields and modular forms of weight 2 and 4.

Putting  $L = (e_L, \mu_L, \tau_L)$  for charged leptons, the charged lepton mass matrix  $M_E^{(k)}$  is given in terms of modular forms of weight 2,  $\mathbf{Y}_3^{(2)}$  or of weight 6,  $\mathbf{Y}_3^{(6)}$  for weight 0 or  $-4$  for right-handed charged leptons, respectively, as:

$$M_E^{(2)} = v_d \begin{pmatrix} \alpha_e & 0 & 0 \\ 0 & \beta_e & 0 \\ 0 & 0 & \gamma_e \end{pmatrix} \begin{pmatrix} Y_1 & Y_3 & Y_2 \\ Y_2 & Y_1 & Y_3 \\ Y_3 & Y_2 & Y_1 \end{pmatrix}_{RL}, \quad (27)$$

$$M_E^{(6)} = v_d \begin{pmatrix} \alpha_e & 0 & 0 \\ 0 & \beta_e & 0 \\ 0 & 0 & \gamma_e \end{pmatrix} \left[ \begin{pmatrix} Y_1^{(6)} & Y_3^{(6)} & Y_2^{(6)} \\ Y_2^{(6)} & Y_1^{(6)} & Y_3^{(6)} \\ Y_3^{(6)} & Y_2^{(6)} & Y_1^{(6)} \end{pmatrix} + g_e \begin{pmatrix} Y_1'^{(6)} & Y_3'^{(6)} & Y_2'^{(6)} \\ Y_2'^{(6)} & Y_1'^{(6)} & Y_3'^{(6)} \\ Y_3'^{(6)} & Y_2'^{(6)} & Y_1'^{(6)} \end{pmatrix} \right]_{RL}, \quad (28)$$

which have the same flavor structure of the down-type quark mass matrix in Eq.(19). Coefficients  $\alpha_e$ ,  $\beta_e$  and  $\gamma_e$  are real parameters while  $g_e$  is complex one.

Suppose neutrinos to be Majorana particles. By using the Weinberg operator, the superpotential of the neutrino mass term,  $w_\nu$  is given as:

$$w_\nu = -\frac{1}{\Lambda} (H_u H_u L L \mathbf{Y}_r^{(k)})_1, \quad (29)$$

where  $\Lambda$  is a relevant cut off scale. Since the left-handed lepton doublet has weight  $-2$ , the superpotential is given in terms of modular forms of weight 4,  $\mathbf{Y}_3^{(4)}$ ,  $\mathbf{Y}_1^{(4)}$  and  $\mathbf{Y}_{1'}^{(4)}$ .

By using the vacuum expectation value of  $H_u$ ,  $v_u$  and putting  $L = (\nu_e, \nu_\mu, \nu_\tau)$  for neutrinos, it is given as:

$$\begin{aligned}
w_\nu &= \frac{v_u^2}{\Lambda} \left[ \begin{pmatrix} 2\nu_e\nu_e - \nu_\mu\nu_\tau - \nu_\tau\nu_\mu \\ 2\nu_\tau\nu_\tau - \nu_e\nu_\mu - \nu_\mu\nu_\tau \\ 2\nu_\mu\nu_\mu - \nu_\tau\nu_e - \nu_e\nu_\tau \end{pmatrix} \otimes \mathbf{Y}_3^{(4)} \right. \\
&\quad \left. + (\nu_e\nu_e + \nu_\mu\nu_\tau + \nu_\tau\nu_\mu) \otimes g_{\nu 1} \mathbf{Y}_1^{(4)} + (\nu_e\nu_\mu + \nu_\mu\nu_e + \nu_\tau\nu_\tau) \otimes g_{\nu 2} \mathbf{Y}_{1'}^{(4)} \right] \\
&= \frac{v_u^2}{\Lambda} \left[ (2\nu_e\nu_e - \nu_\mu\nu_\tau - \nu_\tau\nu_\mu) Y_1^{(4)} + (2\nu_\tau\nu_\tau - \nu_e\nu_\mu - \nu_\mu\nu_e) Y_3^{(4)} + (2\nu_\mu\nu_\mu - \nu_\tau\nu_e - \nu_e\nu_\tau) Y_2^{(4)} \right. \\
&\quad \left. + (\nu_e\nu_e + \nu_\mu\nu_\tau + \nu_\tau\nu_\mu) g_{\nu 1} \mathbf{Y}_1^{(4)} + (\nu_e\nu_\mu + \nu_\mu\nu_e + \nu_\tau\nu_\tau) g_{\nu 2} \mathbf{Y}_{1'}^{(4)} \right], \quad (30)
\end{aligned}$$

where  $\mathbf{Y}_3^{(4)}$ ,  $\mathbf{Y}_1^{(4)}$  and  $\mathbf{Y}_{1'}^{(4)}$  are given in Eq.(13), and  $g_{\nu 1}$ ,  $g_{\nu 2}$  are complex parameters. The neutrino mass matrix is written as follows:

$$M_\nu = \frac{v_u^2}{\Lambda} \left[ \begin{pmatrix} 2Y_1^{(4)} & -Y_3^{(4)} & -Y_2^{(4)} \\ -Y_3^{(4)} & 2Y_2^{(4)} & -Y_1^{(4)} \\ -Y_2^{(4)} & -Y_1^{(4)} & 2Y_3^{(4)} \end{pmatrix} + g_{\nu 1} \mathbf{Y}_1^{(4)} \begin{pmatrix} 1 & 0 & 0 \\ 0 & 0 & 1 \\ 0 & 1 & 0 \end{pmatrix} + g_{\nu 2} \mathbf{Y}_{1'}^{(4)} \begin{pmatrix} 0 & 1 & 0 \\ 1 & 0 & 0 \\ 0 & 0 & 1 \end{pmatrix} \right]_{LL}. \quad (31)$$

Model parameters are  $\alpha_e$ ,  $\beta_e$ ,  $\gamma_e$ ,  $(g_e)$ ,  $g_{\nu 1}$  and  $g_{\nu 2}$ . Parameters  $\alpha_e$ ,  $\beta_e$  and  $\gamma_e$  are adjusted by the observed charged lepton masses as given in Appendix B. Therefore, the lepton mixing angles, the Dirac phase and Majorana phases are given by  $g_{\nu 1}$ ,  $(g_e)$  and  $g_{\nu 2}$  in addition to the value of  $\tau$ . Since  $\tau$  is restricted in the narrow range for the quark sector, we expect to get distinct predictions in the lepton mixing.

## 5.2 Numerical results of leptons

We input charged lepton masses in order to constrain the model parameters. We take Yukawa couplings of charged leptons at the GUT scale  $2 \times 10^{16}$  GeV, where  $\tan \beta = 5$  is taken as well as quark Yukawa couplings [51, 52]:

$$y_e = (1.97 \pm 0.024) \times 10^{-6}, \quad y_\mu = (4.16 \pm 0.050) \times 10^{-4}, \quad y_\tau = (7.07 \pm 0.073) \times 10^{-3}, \quad (32)$$

where lepton masses are given by  $m_\ell = y_\ell v_H$  with  $v_H = 174$  GeV. We also use the following lepton mixing angles and neutrino mass parameters, which are given by NuFit 4.0 in Table 8 [54]. Since there are two possible spectrum of neutrinos masses  $m_i$ , which are the normal hierarchy (NH),  $m_3 > m_2 > m_1$ , and the inverted hierarchy (IH),  $m_2 > m_1 > m_3$ , we investigate both cases.

Neutrino masses and the PMNS matrix  $U_{\text{PMNS}}$  [55, 56] are obtained by diagonalizing  $M_E^{(k)\dagger} M_E^{(k)}$  and  $M_\nu^* M_\nu$ . We also investigate the sum of three neutrino masses  $\sum m_i$  in our model since it is constrained by the recent cosmological data, 120meV [57]. The effective mass for the  $0\nu\beta\beta$  decay is given as follows:

$$\langle m_{ee} \rangle = \left| m_1 c_{12}^2 c_{13}^2 + m_2 s_{12}^2 c_{13}^2 e^{i\alpha_{21}} + m_3 s_{13}^2 e^{i(\alpha_{31} - 2\delta_{CP}^\ell)} \right|, \quad (33)$$

observable	$3\sigma$ range for NH	$3\sigma$ range for IH
$\Delta m_{\text{atm}}^2$	$(2.431\text{--}2.622) \times 10^{-3} \text{eV}^2$	$-(2.413\text{--}2.606) \times 10^{-3} \text{eV}^2$
$\Delta m_{\text{sol}}^2$	$(6.79\text{--}8.01) \times 10^{-5} \text{eV}^2$	$(6.79\text{--}8.01) \times 10^{-5} \text{eV}^2$
$\sin^2 \theta_{23}$	0.428–0.624	0.433–0.623
$\sin^2 \theta_{12}$	0.275–0.350	0.275–0.350
$\sin^2 \theta_{13}$	0.02044–0.02437	0.02067–0.02461

Table 8: The  $3\sigma$  ranges of neutrino parameters from NuFIT 4.0 for NH and IH [54].

where  $\alpha_{21}$  and  $\alpha_{31}$  are Majorana phases as seen in Appendix C.

Let us discuss numerical result for the case of the charged lepton mass matrix  $M_E^{(2)}$  of Eq.(27) in NH of neutrino masses. At first, we show the allowed region  $\text{Re}[\tau]$ – $\text{Im}[\tau]$  plane in Fig.5. Observed three mixing angles of leptons are reproduced at green, blue and red points while observed CKM elements are obtained at brown points for model-I of quarks and magenta points for model-III of quarks, respectively. Especially, both observed quark CKM elements and lepton mixing angles are reproduced at red points.

It is remarked that there are four common regions of  $\tau$  of quarks and leptons only for model-I. Thus, the common  $\tau$  of quarks (model-I) and leptons can give both CKM parameters ( $|V_{us}|$ ,  $|V_{cb}|$ ,  $|V_{ub}|$ ,  $\delta_{CP}$ ), and PMNS mixing angles ( $\theta_{12}$ ,  $\theta_{23}$ ,  $\theta_{13}$ ), which are consistent with experimental data. There is no common  $\tau$  of quarks and leptons for model-III of quarks. The common value of  $\tau$  is restricted in very narrow range as seen in Fig.5. This situation is understandable by taking account of the number of parameters of our model. We have four complex parameters  $\tau$ ,  $g_u$ ,  $g_{\nu 1}$  and  $g_{\nu 2}$  after inputting quarks and charged lepton masses in the framework of model-I of quarks and the charged lepton mass matrix  $M_E^{(2)}$ . These four complex parameters are constrained by eight observed quantities; the four observed CKM elements, three mixing angles of leptons and observed mass ratio  $\Delta m_{\text{sol}}^2/\Delta m_{\text{atm}}^2$ , namely,  $\tau$  is almost determined by the experimental data. Therefore, we can predict distinctly the CP violating phase  $\delta_{CP}^\ell$ , Majorana phases  $\alpha_{21}$ ,  $\alpha_{31}$ , the effective mass  $\langle m_{ee} \rangle$  for the  $0\nu\beta\beta$  decay and the sum of neutrino masses.

We show the predicted  $\delta_{CP}^\ell$  versus  $\sin^2 \theta_{23}$  in Fig.6, where colors of points correspond to points of  $\tau$  in Fig.5. Red points denote common values of  $\tau$  in both quark and lepton mass matrices. At the red point region, we predict  $\delta_{CP}^\ell = 100^\circ\text{--}120^\circ$  and  $240^\circ\text{--}260^\circ$  while  $\sin^2 \theta_{23} = 0.46\text{--}0.47$ . It is

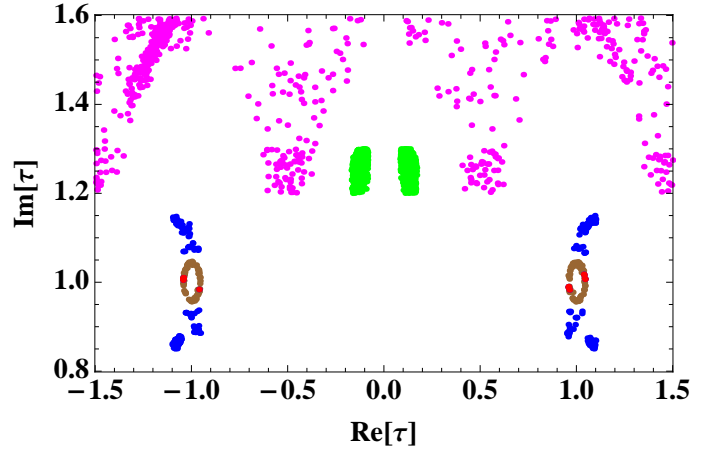


Figure 5: The allowed region on  $\text{Re}[\tau]$ – $\text{Im}[\tau]$  plane for  $M_E^{(2)}$  in the case of NH. Observed three mixing angles of leptons are reproduced at green, blue and red points while observed CKM elements are reproduced at brown points and magenta points in model-I and model-III, respectively. Both quark CKM elements and lepton mixing angles are reproduced at red points.

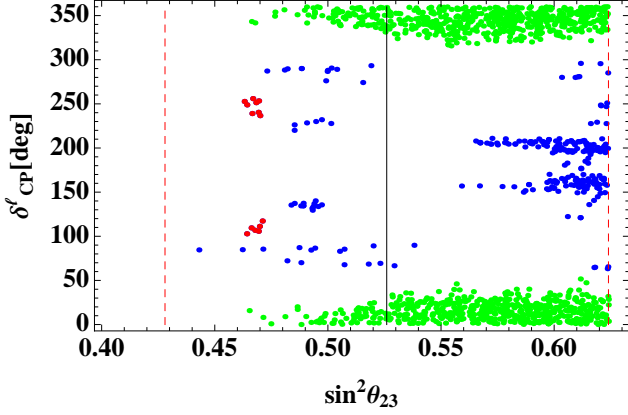


Figure 6: Predicted  $\delta_{CP}^\ell$  versus  $\sin^2 \theta_{23}$ , where black line denotes observed central value of  $\sin^2 \theta_{23}$ , and red dashed-lines denote its upper(lower)-bound of  $3\sigma$  interval for  $M_E^{(2)}$  in the case of NH. Colors of points correspond to points of  $\tau$  in Fig.5. At red points, the common  $\tau$  is realized in leptons and quarks of model-I.

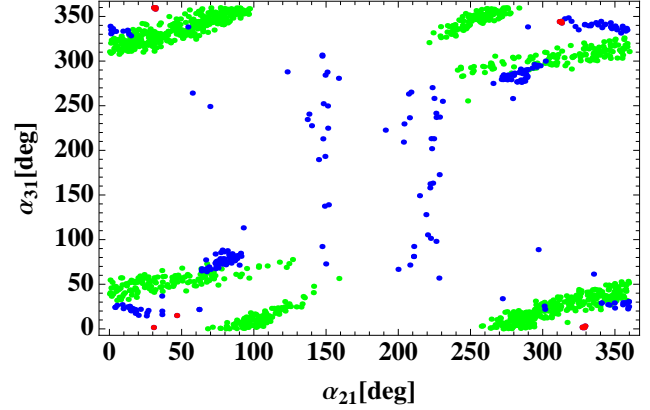


Figure 7: Predicted region of Majorana phases in the  $\alpha_{21}$ - $\alpha_{31}$  plane, for  $M_E^{(2)}$  in the case of NH. Colors of points correspond to points of  $\tau$  in Fig.5. At red points, the common  $\tau$  is realized in leptons and quarks of model-I.

noticed that the predicted regions are rather broad (green and blue points) without inputs of CKM parameters of the quark sector. Thus, the common  $\tau$  gives the distinct predictions for  $\sin^2 \theta_{23}$  and  $\delta_{CP}^\ell$ . The observed  $\sin^2 \theta_{23}$  should be lower than  $1/2$ , namely, in the first octant. On the other hand, the absolute value of  $\sin \delta_{CP}^\ell$  is  $0.87$ – $0.98$ , but its sign is still undetermined. These predictions will be tested in the near future neutrino experiments.

We also present the prediction of Majorana phases on the  $\alpha_{21}$ - $\alpha_{31}$  plane in Fig.7. At the red point region, we obtain four regions of  $(\alpha_{21}, \alpha_{31}) \simeq (30^\circ - 50^\circ, 0^\circ - 10^\circ)$ ,  $(30^\circ, 360^\circ)$ ,  $(330^\circ, 0^\circ)$ ,  $(310^\circ, 350^\circ)$  although the predicted region is rather broad without inputs of CKM parameters of the

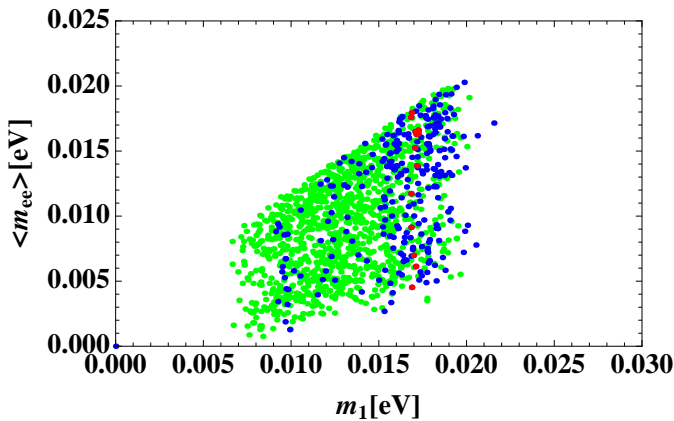


Figure 8: Predicted effective mass  $\langle m_{ee} \rangle$  of the  $0\nu\beta\beta$  decay versus  $m_1$  for  $M_E^{(2)}$  in the case of NH. Red points have common  $\tau$  in leptons and quarks of model-I.

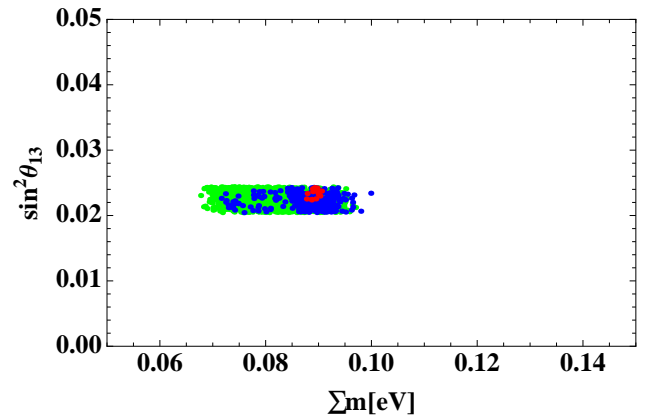


Figure 9: Sum of masses and  $\sin^2 \theta_{13}$  for  $M_E^{(2)}$  in the case of NH, where  $\sin^2 \theta_{13}$  is presented within observed  $3\sigma$  interval. Red points have common  $\tau$  in leptons and quarks of model-I.



quark sector.

By using these Majorana phases, we can predict the effective mass  $\langle m_{ee} \rangle$  for the  $0\nu\beta\beta$  decay versus the lightest mass  $m_1$  as seen in Fig.8. We obtain  $\langle m_{ee} \rangle = 4\text{--}18\text{meV}$  and  $m_1 \simeq 17\text{meV}$ , which may be tested in the future experiments.

We also show  $\sin^2 \theta_{13}$  versus the sum of neutrino masses  $\sum m_i$  in Fig.9. At the red point region, we obtain  $\sin^2 \theta_{13} = 0.022\text{--}0.024$  and  $\sum m_i \simeq 90\text{meV}$ , which are compared with the observed one  $\sin^2 \theta_{13} = 0.02044\text{--}0.02437$  in Table 8 and the cosmological upper-bound of the sum of neutrino masses  $120\text{meV}$ . The figure of the calculated  $\sin^2 \theta_{12}$  is omitted in this paper. At red points of  $\tau$ , it is distributed in the overall range of the experimental data with  $3\sigma$  error-bar.

Next, we discuss numerical result for the case of the charged lepton mass matrix  $M_E^{(6)}$  of Eq.(28) for NH of neutrino masses with keeping the neutrino mass matrix in Eq.(31). We show the allowed region on the  $\text{Re}[\tau]\text{--}\text{Im}[\tau]$  plane, where PMNS mixing angles  $\theta_{12}$ ,  $\theta_{23}$  and  $\theta_{13}$  are consistent with experimental data for NH of neutrino masses, in Fig.10. Observed three mixing angles of leptons are reproduced at green, blue and red points while observed CKM elements are obtained at brown points for model-I of quarks and magenta points for model-III of quarks, respectively. It is noted that blue and red points almost overlap. There are two common regions of  $\tau$  of quarks and leptons only for model-I as well as in for the case of the charged lepton mass matrix  $M_E^{(2)}$ .

We show the predicted  $\delta_{CP}^\ell$  versus  $\sin^2 \theta_{23}$  in Fig.11, where colors of points correspond to points of  $\tau$  in Fig.10. Red points denote common values of  $\tau$  in both quark and lepton mass matrices. At the red point region, we predict  $\delta_{CP}^\ell = 170^\circ\text{--}190^\circ$  and  $\sin^2 \theta_{23} = 0.428\text{--}0.51$ . The predicted CP violating Dirac phase  $\delta_{CP}^\ell$  around  $180^\circ$  may be inconsistent with recent observation of the CP violation at T2K and NO $\nu$ A experiments [39, 40].

We also present the prediction of Majorana phases on the  $\alpha_{21}\text{--}\alpha_{31}$  plane in Fig.12. At the red point region, we obtain  $(\alpha_{21}, \alpha_{31}) \simeq (90^\circ\text{--}140^\circ, 10^\circ\text{--}40^\circ)$  and  $(220^\circ\text{--}270^\circ, 330^\circ\text{--}360^\circ)$ .

By using these Majorana phases, we can predict the effective mass  $\langle m_{ee} \rangle$  for the  $0\nu\beta\beta$  decay versus the lightest mass  $m_1$  as seen in Fig.13. The predicted  $\langle m_{ee} \rangle = 6\text{--}31\text{meV}$  is rather broad while  $m_1$  is  $24\text{--}32\text{meV}$ .

We show  $\sin^2 \theta_{13}$  versus the sum of neutrino masses  $\sum m_i$  in Fig.14. At the red point region, we obtain  $\sum m_i = 105\text{--}125\text{meV}$ , which is close to the cosmological upper-bound  $120\text{meV}$ , while  $\sin^2 \theta_{13}$  covers all region of the observation with  $3\sigma$  error-bar in Table 8. The presentation of the calculated  $\sin^2 \theta_{12}$  is also omitted since it is distributed in the overall range of the experimental data with  $3\sigma$  error-bar at red points of the modulus  $\tau$ . Thus, our predictions for both  $M_E^{(2)}$  and  $M_E^{(6)}$  are distinguished ones compared with other flavor models because the quark CKM matrix

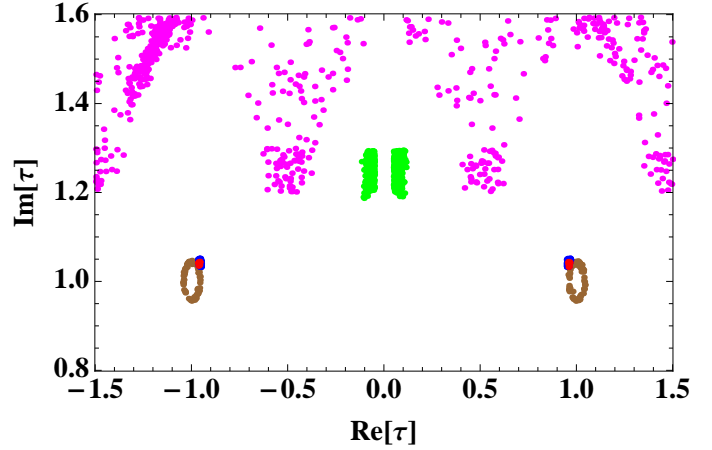


Figure 10: Allowed region on  $\text{Re}[\tau]\text{--}\text{Im}[\tau]$  plane for  $M_E^{(6)}$  in the case of NH. Observed mixing angles of leptons are reproduced at green, blue and red points while CKM elements are reproduced at brown and magenta points in model-I and model-III, respectively. Both quark CKM elements and lepton mixing angles are reproduced at red points.



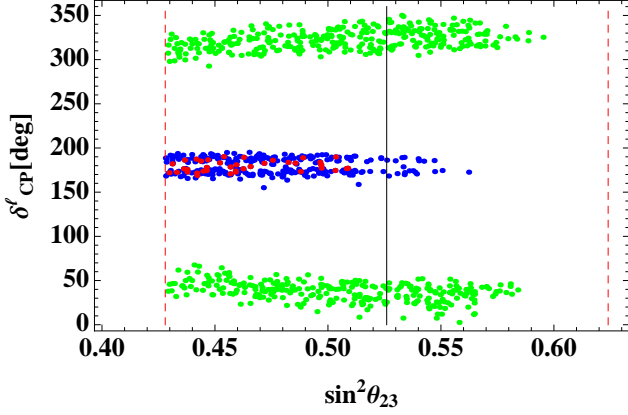


Figure 11: Predicted  $\delta'_{CP}$  versus  $\sin^2\theta_{23}$ , where black line denotes observed central value of  $\sin^2\theta_{23}$ , and red dashed-lines denote its upper(lower)-bound of  $3\sigma$  interval for  $M_E^{(6)}$  in the case of NH. Colors of points correspond to points of  $\tau$  in Fig.5. At red points, the common  $\tau$  is realized in leptons and quarks of model-I.

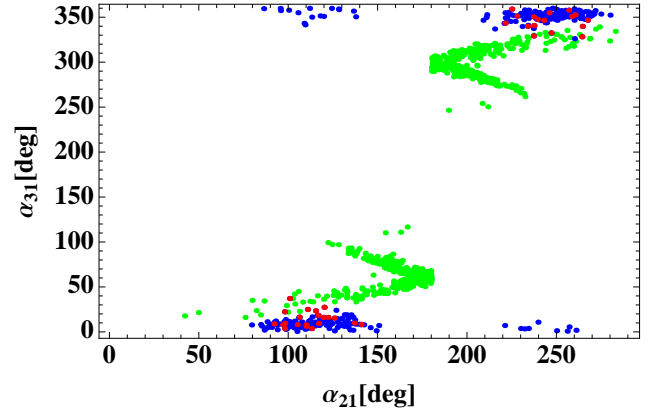


Figure 12: Predicted region of Majorana phases in the  $\alpha_{21}$ - $\alpha_{31}$  plane, for  $M_E^{(6)}$  in the case of NH. Colors of points correspond to points of  $\tau$  in Fig.10. At red points, the common  $\tau$  is realized in leptons and quarks of model-I.

provides severe a constraint for the value of modulus  $\tau$ .

In our numerical calculations, we have not included the RGE effects in the lepton mixing angles and neutrino mass ratio  $\Delta m_{\text{sol}}^2/\Delta m_{\text{atm}}^2$ . We suppose that those corrections are very small between EW and GUT scales for NH of neutrino masses. This assumption is justified well in the case of  $\tan\beta \leq 5$  unless neutrino masses are almost degenerate [26].

In Table 9, we show typical parameter sets, calculated lepton mixing angles and the Dirac CP phase for the case of the charged lepton mass matrix of  $M_E^{(2)}$  and  $M_E^{(6)}$ , respectively. It is noticed that ratios of  $\alpha_e/\gamma_e$  and  $\beta_e/\gamma_e$  in Table 9 correspond to the observed charged lepton mass hierarchy.

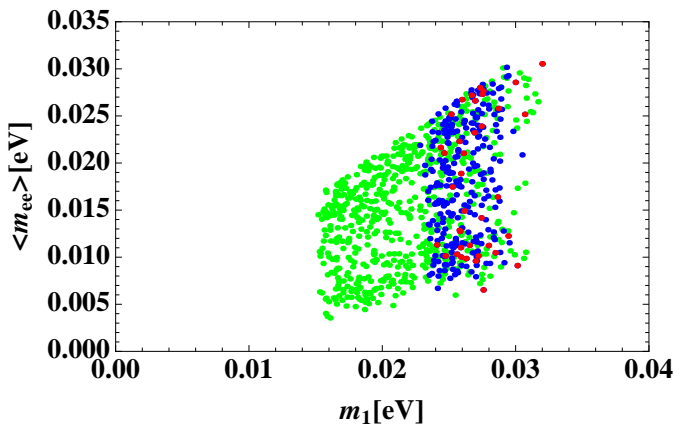


Figure 13: Predicted effective mass  $\langle m_{ee} \rangle$  of the  $0\nu\beta\beta$  decay versus  $m_1$  for  $M_E^{(6)}$  in the case of NH. Red points have the common  $\tau$  in leptons and quarks of model-I.

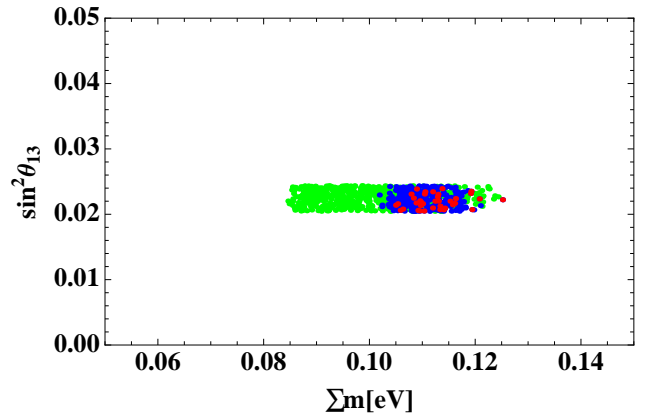


Figure 14: Sum of masses and  $\sin^2\theta_{13}$  for  $M_E^{(6)}$  in the case of NH, where  $\sin^2\theta_{13}$  is presented within observed  $3\sigma$  interval. Red points have common  $\tau$  in leptons and quarks of model-I.

	$M_E^{(2)}$	$M_E^{(6)}$
$\tau$	$1.045 + 1.007 i$	$0.958 + 1.038 i$
$g_{\nu 1}$	$0.891 - 0.129 i$	$0.725 - 0.027 i$
$g_{\nu 2}$	$-0.468 + 0.190 i$	$0.765 + 0.071 i$
$g_e$	—	$0.446 - 0.018 i$
$\alpha_e/\gamma_e$	0.0261	28.7
$\beta_e/\gamma_e$	14.7	427
$\sin \theta_{12}^2$	0.333	0.296
$\sin \theta_{23}^2$	0.467	0.446
$\sin \theta_{13}^2$	0.0237	0.0209
$\delta_{CP}^\ell$	$256^\circ$	$174^\circ$

Table 9: Numerical values of parameters and output of PMNS parameters at the sample points for charged lepton mass matrices  $M_E^{(2)}$  and  $M_E^{(6)}$ , respectively.

It is also remarked that the large CP violating phase  $\delta_{CP}^\ell$  is mainly originated from  $\text{Re}[\tau]$ . Indeed, we have checked that the contributions of the imaginary parts of  $g_{\nu 1}$ ,  $g_{\nu 2}$  and  $g_e$  to  $\delta_{CP}^\ell$  are minor.

We also present the mixing matrices of charged leptons and neutrinos for the two samples in order to investigate the flavor structure of those mass matrices. For the sample of  $M_E^{(2)}$  in Table 9, we obtain

$$|U_\ell| = \begin{pmatrix} 0.594 & 0.566 & 0.572 \\ 0.571 & 0.211 & 0.794 \\ 0.567 & 0.797 & 0.208 \end{pmatrix}, \quad |U_\nu| = \begin{pmatrix} 0.443 & 0.361 & 0.820 \\ 0.071 & 0.900 & 0.429 \\ 0.894 & 0.243 & 0.377 \end{pmatrix}, \quad (34)$$

where  $U_{\text{PMNS}} = U_\ell^\dagger U_\nu$ . For the sample of  $M_E^{(6)}$  in Table 9, we have

$$|U_\ell| = \begin{pmatrix} 0.578 & 0.393 & 0.715 \\ 0.551 & 0.458 & 0.698 \\ 0.602 & 0.797 & 0.048 \end{pmatrix}, \quad |U_\nu| = \begin{pmatrix} 0.472 & 0.245 & 0.847 \\ 0.117 & 0.964 & 0.240 \\ 0.874 & 0.105 & 0.475 \end{pmatrix}. \quad (35)$$

It is noticed that the flavor structure of lepton mass matrices is anarchy for both cases of  $M_E^{(2)}$  and  $M_E^{(6)}$ . The observed PMNS matrix is realized by the relevant cancellation between the charged lepton and neutrino mass matrices.

Finally, we discuss briefly the case of IH of neutrino masses. The observed three mixing angles cannot be reproduced for arbitrary value of  $\tau$  for both  $M_E^{(2)}$  and  $M_E^{(6)}$ . It is impossible to realize  $\sin^2 \theta_{13} \leq 0.1$  while  $\theta_{12}$  and  $\theta_{23}$  keep observed values. In conclusion, the case of IH of neutrino masses is excluded in our lepton mass matrices.

## 6 Summary

In this work, we have studied both quarks and leptons in the  $A_4$  modular symmetry towards the unification of quark and lepton flavors. If flavors of quarks and leptons are originated from a

same two-dimensional compact space, the quarks and leptons have same flavor symmetry and the same value of the modulus  $\tau$ . For the quark sector and the charged lepton one, we have adopted modular forms of weights 2 and 6, on the other hand, we have used modular forms of weight 4 for the neutrino mass matrix generated by the Weinberg operator. We have presented the viable two models for quark mass matrices. The first one (model-I) is that the down-type quark mass matrix is constructed by modular forms of weight 2, but the up-type quark mass matrix is constructed by modular forms of weight 6. Another one (model-III) is that both quark mass matrices are given by modular forms of weight 6. We have also discussed charged lepton mass matrices which are constructed by modular forms of weights 2 and 6, respectively. On the other hands, the neutrino mass matrix is given by modular forms of weight 4.

It is found that the model-I of quarks works well together with the lepton models on the common modulus  $\tau$ , on the other hand, the model-III of quarks does not work. Imposing the allowed value of the modulus  $\tau$  of model-I in addition to the observed three mixing angles of leptons and the neutrino mass ratio  $\Delta m_{\text{sol}}^2/\Delta m_{\text{atm}}^2$ , the model parameters of leptons are almost fixed. Therefore, the CP violating phase and sum of neutrino masses are predicted distinctly. For the charged lepton mass matrix constructed by modular forms of weight 2,  $\sin^2 \theta_{23}$  is predicted as 0.46–0.47, and the CP violating Dirac phase is  $\delta_{CP}^\ell = 100^\circ\text{--}120^\circ$  or  $240^\circ\text{--}260^\circ$  in the case of NH of neutrino masses. This large CP violating phase is mainly originated from the modulus  $\tau$ . The effective neutrino mass is  $\langle m_{ee} \rangle = 4\text{--}18\text{meV}$ . The sum of neutrino masses is 90meV. These predictions will be tested in the near future neutrino experiments.

For the charged lepton mass matrix constructed by modular forms of weight 6,  $\sin^2 \theta_{23}$  is predicted as 0.43–0.51, and the CP violating Dirac phase is  $\delta_{CP}^\ell = 170^\circ\text{--}190^\circ$  in the case of NH of neutrino masses. The effective neutrino mass is  $\langle m_{ee} \rangle = 6\text{--}31\text{meV}$ . The sum of neutrino masses is 105–125meV. The prediction of  $\delta_{CP}^\ell$  may be inconsistent with recent observation of the CP violation at T2K and NO $\nu$ A experiments [39, 40].

It is remarked that the IH neutrino mass spectrum is not allowed in our scheme of the modular invariance.

Our study provides a new aspect of the unification of the quark and lepton flavors in terms of the modulus  $\tau$ .

## Acknowledgments

This research is supported by the Ministry of Science, ICT and Future Planning, Gyeongsangbuk-do and Pohang City (H.O.). H. O. is sincerely grateful for KIAS and all the members.

## Appendix

### A Tensor product of $A_4$ group

We take the generators of  $A_4$  group as follows:

$$S = \frac{1}{3} \begin{pmatrix} -1 & 2 & 2 \\ 2 & -1 & 2 \\ 2 & 2 & -1 \end{pmatrix}, \quad T = \begin{pmatrix} 1 & 0 & 0 \\ 0 & \omega & 0 \\ 0 & 0 & \omega^2 \end{pmatrix}, \quad (36)$$

where  $\omega = e^{i\frac{2}{3}\pi}$  for a triplet. In this base, the multiplication rule of the  $A_4$  triplet is

$$\begin{aligned} \begin{pmatrix} a_1 \\ a_2 \\ a_3 \end{pmatrix}_{\mathbf{3}} \otimes \begin{pmatrix} b_1 \\ b_2 \\ b_3 \end{pmatrix}_{\mathbf{3}} &= (a_1 b_1 + a_2 b_3 + a_3 b_2)_{\mathbf{1}} \oplus (a_3 b_3 + a_1 b_2 + a_2 b_1)_{\mathbf{1}'} \\ &\quad \oplus (a_2 b_2 + a_1 b_3 + a_3 b_1)_{\mathbf{1}''} \\ &\quad \oplus \frac{1}{3} \begin{pmatrix} 2a_1 b_1 - a_2 b_3 - a_3 b_2 \\ 2a_3 b_3 - a_1 b_2 - a_2 b_1 \\ 2a_2 b_2 - a_1 b_3 - a_3 b_1 \end{pmatrix}_{\mathbf{3}} \oplus \frac{1}{2} \begin{pmatrix} a_2 b_3 - a_3 b_2 \\ a_1 b_2 - a_2 b_1 \\ a_3 b_1 - a_1 b_3 \end{pmatrix}_{\mathbf{3}} , \end{aligned}$$

$$\mathbf{1} \otimes \mathbf{1} = \mathbf{1} , \quad \mathbf{1}' \otimes \mathbf{1}' = \mathbf{1}'' , \quad \mathbf{1}'' \otimes \mathbf{1}'' = \mathbf{1}' , \quad \mathbf{1}' \otimes \mathbf{1}'' = \mathbf{1} . \quad (37)$$

More details are shown in the review [6, 7].

## B $\alpha_q/\gamma_q$ and $\beta_q/\gamma_q$ in terms of quark masses

The coefficients  $\alpha_q$ ,  $\beta_q$ , and  $\gamma_q$  in Eqs.(17) and (18) are taken to be real positive without loss of generality. These parameters are described in terms of the modulus  $\tau$  and quark masses. As a representative, we examine the quark mass matrix in Eq. (18) as follows:

$$M_q = v_q \gamma_q \begin{pmatrix} \hat{\alpha}_q & 0 & 0 \\ 0 & \hat{\beta}_q & 0 \\ 0 & 0 & 1 \end{pmatrix} \left[ \begin{pmatrix} Y_1^{(6)} & Y_3^{(6)} & Y_2^{(6)} \\ Y_2^{(6)} & Y_1^{(6)} & Y_3^{(6)} \\ Y_3^{(6)} & Y_2^{(6)} & Y_1^{(6)} \end{pmatrix} + g_q \begin{pmatrix} Y_1'^{(6)} & Y_3'^{(6)} & Y_2'^{(6)} \\ Y_2'^{(6)} & Y_1'^{(6)} & Y_3'^{(6)} \\ Y_3'^{(6)} & Y_2'^{(6)} & Y_1'^{(6)} \end{pmatrix} \right]_{RL} , \quad (q = u \text{ or } d) , \quad (38)$$

where  $\hat{\alpha}_q \equiv \alpha_q/\gamma_q$  and  $\hat{\beta}_q \equiv \beta_q/\gamma_q$ . Then, we have three equations as:

$$\sum_{i=1}^3 m_{q_i}^2 = \text{Tr}[M_q^\dagger M_q] = v_q^2 \gamma_q^2 (1 + \hat{\alpha}_q^2 + \hat{\beta}_q^2) C_1^q , \quad (39)$$

$$\prod_{i=1}^3 m_{q_i}^2 = \text{Det}[M_q^\dagger M_q] = v_q^6 \gamma_q^6 \hat{\alpha}_q^2 \hat{\beta}_q^2 C_2^q , \quad (40)$$

$$\chi = \frac{\text{Tr}[M_q^\dagger M_q]^2 - \text{Tr}[(M_q^\dagger M_q)^2]}{2} = v_q^4 \gamma_q^4 (\hat{\alpha}_q^2 + \hat{\alpha}_q^2 \hat{\beta}_q^2 + \hat{\beta}_q^2) C_3^q , \quad (41)$$

where  $\chi \equiv m_{q_1}^2 m_{q_2}^2 + m_{q_2}^2 m_{q_3}^2 + m_{q_3}^2 m_{q_1}^2$ . The coefficients  $C_1^q$ ,  $C_2^q$ , and  $C_3^q$  depend only on  $Y_i^{(6)}$ ,  $Y_i'^{(6)}$  and  $g_q$ , where  $Y_i^{(6)}$  and  $Y_i'^{(6)}$  are determined if the value of modulus  $\tau$  is fixed, and  $g_q$  is an arbitrary complex coefficient. Those are given explicitly as follows:

$$C_1^q = |\tilde{Y}_1|^2 + |\tilde{Y}_2|^2 + |\tilde{Y}_3|^2 ,$$

$$C_2^q = |\tilde{Y}_1^3 + \tilde{Y}_2^3 + \tilde{Y}_3^3 - 3\tilde{Y}_1\tilde{Y}_2\tilde{Y}_3|^2 ,$$

$$C_3^q = |\tilde{Y}_1|^4 + |\tilde{Y}_2|^4 + |\tilde{Y}_3|^4 + |\tilde{Y}_1\tilde{Y}_2|^2 + |\tilde{Y}_2\tilde{Y}_3|^2 + |\tilde{Y}_1\tilde{Y}_3|^2 - 2\text{Re} \left[ \tilde{Y}_1^* \tilde{Y}_2^* \tilde{Y}_3^2 + \tilde{Y}_1^2 \tilde{Y}_2^* \tilde{Y}_3^* + \tilde{Y}_1^* \tilde{Y}_2^2 \tilde{Y}_3^* \right] ,$$

where  $\tilde{Y}_i \equiv Y_i^{(6)} + g_q Y_i'^{(6)}$  ( $i = 1, 2, 3$ ).

Then, we obtain two equations which describe  $\hat{\alpha}$  and  $\hat{\beta}$  as forms of quark masses,  $\tau$  and  $g_q$ :

$$\frac{(1+s)(s+t)}{t} = \frac{(\sum m_i^2/C_1^q)(\chi/C_3^q)}{\prod m_i^2/C_2^q}, \quad \frac{(1+s)^2}{s+t} = \frac{(\sum m_i^2/C_1^q)^2}{\chi/C_3^q}, \quad (42)$$

where we redefine the parameters  $\hat{\alpha}_q^2 + \hat{\beta}_q^2 = s$  and  $\hat{\alpha}_q^2 \hat{\beta}_q^2 = t$ . They are related as follows:

$$\hat{\alpha}_q^2 = \frac{s \pm \sqrt{s^2 - 4t}}{2}, \quad \hat{\beta}_q^2 = \frac{s \mp \sqrt{s^2 - 4t}}{2}. \quad (43)$$

## C Majorana and Dirac phases and $\langle m_{ee} \rangle$ in $0\nu\beta\beta$ decay

Supposing neutrinos to be Majorana particles, the PMNS matrix  $U_{\text{PMNS}}$  [55, 56] is parametrized in terms of the three mixing angles  $\theta_{ij}$  ( $i, j = 1, 2, 3$ ;  $i < j$ ), one CP violating Dirac phase  $\delta_{\text{CP}}$  and two Majorana phases  $\alpha_{21}, \alpha_{31}$  as follows:

$$U_{\text{PMNS}} = \begin{pmatrix} c_{12}c_{13} & s_{12}c_{13} & s_{13}e^{-i\delta_{\text{CP}}^\ell} \\ -s_{12}c_{23} - c_{12}s_{23}s_{13}e^{i\delta_{\text{CP}}^\ell} & c_{12}c_{23} - s_{12}s_{23}s_{13}e^{i\delta_{\text{CP}}^\ell} & s_{23}c_{13} \\ s_{12}s_{23} - c_{12}c_{23}s_{13}e^{i\delta_{\text{CP}}^\ell} & -c_{12}s_{23} - s_{12}c_{23}s_{13}e^{i\delta_{\text{CP}}^\ell} & c_{23}c_{13} \end{pmatrix} \begin{pmatrix} 1 & 0 & 0 \\ 0 & e^{i\frac{\alpha_{21}}{2}} & 0 \\ 0 & 0 & e^{i\frac{\alpha_{31}}{2}} \end{pmatrix}, \quad (44)$$

where  $c_{ij}$  and  $s_{ij}$  denote  $\cos \theta_{ij}$  and  $\sin \theta_{ij}$ , respectively.

The rephasing invariant CP violating measure of leptons [58, 59] is defined by the PMNS matrix elements  $U_{\alpha i}$ . It is written in terms of the mixing angles and the CP violating phase as:

$$J_{CP} = \text{Im} [U_{e1}U_{\mu 2}U_{e2}^*U_{\mu 1}^*] = s_{23}c_{23}s_{12}c_{12}s_{13}c_{13}^2 \sin \delta_{\text{CP}}^\ell, \quad (45)$$

where  $U_{\alpha i}$  denotes the each component of the PMNS matrix.

There are also other invariants  $I_1$  and  $I_2$  associated with Majorana phases

$$I_1 = \text{Im} [U_{e1}^*U_{e2}] = c_{12}s_{12}c_{13}^2 \sin \left( \frac{\alpha_{21}}{2} \right), \quad I_2 = \text{Im} [U_{e1}^*U_{e3}] = c_{12}s_{13}c_{13} \sin \left( \frac{\alpha_{31}}{2} - \delta_{\text{CP}}^\ell \right). \quad (46)$$

We can calculate  $\delta_{\text{CP}}^\ell$ ,  $\alpha_{21}$  and  $\alpha_{31}$  with these relations by taking account of

$$\cos \delta_{CP}^\ell = \frac{|U_{\tau 1}|^2 - s_{12}^2 s_{23}^2 - c_{12}^2 c_{23}^2 s_{13}^2}{2c_{12}s_{12}c_{23}s_{23}s_{13}}, \quad \text{Re} [U_{e1}^*U_{e2}] = c_{12}s_{12}c_{13}^2 \cos \left( \frac{\alpha_{21}}{2} \right), \quad \text{Re} [U_{e1}^*U_{e3}] = c_{12}s_{13}c_{13} \cos \left( \frac{\alpha_{31}}{2} - \delta_{\text{CP}}^\ell \right). \quad (47)$$

In terms of these parametrization, the effective mass for the  $0\nu\beta\beta$  decay is given as follows:

$$\langle m_{ee} \rangle = \left| m_1 c_{12}^2 c_{13}^2 + m_2 s_{12}^2 c_{13}^2 e^{i\alpha_{21}} + m_3 s_{13}^2 e^{i(\alpha_{31} - 2\delta_{CP}^\ell)} \right|. \quad (48)$$

## References

- [1] S. Pakvasa and H. Sugawara, Phys. Lett. **73B** (1978) 61.
- [2] F. Wilczek and A. Zee, Phys. Lett. **70B** (1977) 418 Erratum: [Phys. Lett. **72B** (1978) 504].
- [3] M. Fukugita, M. Tanimoto and T. Yanagida, Phys. Rev. D **57** (1998) 4429 [hep-ph/9709388].
- [4] Y. Fukuda *et al.* [Super-Kamiokande Collaboration], Phys. Rev. Lett. **81** (1998) 1562 [hep-ex/9807003].
- [5] G. Altarelli and F. Feruglio, Rev. Mod. Phys. **82** (2010) 2701 [arXiv:1002.0211 [hep-ph]].
- [6] H. Ishimori, T. Kobayashi, H. Ohki, Y. Shimizu, H. Okada and M. Tanimoto, Prog. Theor. Phys. Suppl. **183** (2010) 1 [arXiv:1003.3552 [hep-th]].
- [7] H. Ishimori, T. Kobayashi, H. Ohki, H. Okada, Y. Shimizu and M. Tanimoto, Lect. Notes Phys. **858** (2012) 1, Springer.
- [8] D. Hernandez and A. Y. Smirnov, Phys. Rev. D **86** (2012) 053014 [arXiv:1204.0445 [hep-ph]].
- [9] S. F. King and C. Luhn, Rept. Prog. Phys. **76** (2013) 056201 [arXiv:1301.1340 [hep-ph]].
- [10] S. F. King, A. Merle, S. Morisi, Y. Shimizu and M. Tanimoto, New J. Phys. **16**, 045018 (2014) doi:10.1088/1367-2630/16/4/045018 [arXiv:1402.4271 [hep-ph]].
- [11] M. Tanimoto, AIP Conf. Proc. **1666** (2015) 120002.
- [12] S. F. King, Prog. Part. Nucl. Phys. **94** (2017) 217 doi:10.1016/j.ppnp.2017.01.003 [arXiv:1701.04413 [hep-ph]].
- [13] S. T. Petcov, Eur. Phys. J. C **78** (2018) no.9, 709 [arXiv:1711.10806 [hep-ph]].
- [14] E. Ma and G. Rajasekaran, Phys. Rev. D **64**, 113012 (2001) [arXiv:hep-ph/0106291].
- [15] K. S. Babu, E. Ma and J. W. F. Valle, Phys. Lett. B **552**, 207 (2003) [arXiv:hep-ph/0206292].
- [16] G. Altarelli and F. Feruglio, Nucl. Phys. B **720** (2005) 64 [hep-ph/0504165].
- [17] G. Altarelli and F. Feruglio, Nucl. Phys. B **741** (2006) 215 [hep-ph/0512103].
- [18] Y. Shimizu, M. Tanimoto and A. Watanabe, Prog. Theor. Phys. **126** (2011) 81 [arXiv:1105.2929 [hep-ph]].
- [19] S. T. Petcov and A. V. Titov, Phys. Rev. D **97** (2018) no.11, 115045 [arXiv:1804.00182 [hep-ph]].
- [20] S. K. Kang, Y. Shimizu, K. Takagi, S. Takahashi and M. Tanimoto, PTEP **2018**, no. 8, 083B01 (2018) doi:10.1093/ptep/pty080 [arXiv:1804.10468 [hep-ph]].
- [21] F. Feruglio, arXiv:1706.08749 [hep-ph].

- [22] R. de Adelhart Toorop, F. Feruglio and C. Hagedorn, Nucl. Phys. B **858**, 437 (2012) [arXiv:1112.1340 [hep-ph]].
- [23] T. Kobayashi, K. Tanaka and T. H. Tatsuishi, Phys. Rev. D **98** (2018) no.1, 016004 [arXiv:1803.10391 [hep-ph]].
- [24] J. T. Penedo and S. T. Petcov, Nucl. Phys. B **939** (2019) 292 [arXiv:1806.11040 [hep-ph]].
- [25] P. P. Novichkov, J. T. Penedo, S. T. Petcov and A. V. Titov, JHEP **1904** (2019) 174 [arXiv:1812.02158 [hep-ph]].
- [26] J. C. Criado and F. Feruglio, SciPost Phys. **5** (2018) no.5, 042 [arXiv:1807.01125 [hep-ph]].
- [27] T. Kobayashi, N. Omoto, Y. Shimizu, K. Takagi, M. Tanimoto and T. H. Tatsuishi, JHEP **1811** (2018) 196 [arXiv:1808.03012 [hep-ph]].
- [28] P. P. Novichkov, J. T. Penedo, S. T. Petcov and A. V. Titov, JHEP **1904** (2019) 005 [arXiv:1811.04933 [hep-ph]].
- [29] G. J. Ding, S. F. King and X. G. Liu, arXiv:1903.12588 [hep-ph].
- [30] F. J. de Anda, S. F. King and E. Perdomo, arXiv:1812.05620 [hep-ph].
- [31] P. P. Novichkov, S. T. Petcov and M. Tanimoto, Phys. Lett. B **793** (2019) 247 [arXiv:1812.11289 [hep-ph]].
- [32] T. Kobayashi and S. Tamba, Phys. Rev. D **99** (2019) no.4, 046001 [arXiv:1811.11384 [hep-th]].
- [33] A. Baur, H. P. Nilles, A. Trautner and P. K. S. Vaudrevange, arXiv:1901.03251 [hep-th].
- [34] P. P. Novichkov, J. T. Penedo, S. T. Petcov and A. V. Titov, arXiv:1905.11970 [hep-ph].
- [35] T. Kobayashi, Y. Shimizu, K. Takagi, M. Tanimoto, T. H. Tatsuishi and H. Uchida, doi:10.1016/j.physletb.2019.05.034 arXiv:1812.11072 [hep-ph].
- [36] H. Okada and M. Tanimoto, Phys. Lett. B **791** (2019) 54 [arXiv:1812.09677 [hep-ph]].
- [37] T. Nomura and H. Okada, arXiv:1904.03937 [hep-ph].
- [38] Y. Kariyazono, T. Kobayashi, S. Takada, S. Tamba and H. Uchida, arXiv:1904.07546 [hep-th].
- [39] K. Abe *et al.* [T2K Collaboration], Phys. Rev. Lett. **121** (2018) no.17, 171802 [arXiv:1807.07891 [hep-ex]].
- [40] P. Adamson *et al.* [NOvA Collaboration], Phys. Rev. Lett. **118** (2017) no.23, 231801 [arXiv:1703.03328 [hep-ex]].
- [41] J. Lauer, J. Mas and H. P. Nilles, Phys. Lett. B **226**, 251 (1989); Nucl. Phys. B **351**, 353 (1991).
- [42] W. Lerche, D. Lust and N. P. Warner, Phys. Lett. B **231**, 417 (1989).

- [43] S. Ferrara, D. Lust and S. Theisen, Phys. Lett. B **233**, 147 (1989).
- [44] D. Cremades, L. E. Ibanez and F. Marchesano, JHEP **0405**, 079 (2004) [hep-th/0404229].
- [45] T. Kobayashi and S. Nagamoto, Phys. Rev. D **96**, no. 9, 096011 (2017) [arXiv:1709.09784 [hep-th]].
- [46] T. Kobayashi, S. Nagamoto, S. Takada, S. Tamba and T. H. Tatsuishi, Phys. Rev. D **97**, no. 11, 116002 (2018) [arXiv:1804.06644 [hep-th]].
- [47] S. Ferrara, D. Lust, A. D. Shapere and S. Theisen, Phys. Lett. B **225**, 363 (1989).
- [48] R. C. Gunning, *Lectures on Modular Forms* (Princeton University Press, Princeton, NJ, 1962).
- [49] B. Schoeneberg, *Elliptic Modular Functions* (Springer-Verlag, 1974).
- [50] N. Koblitz, *Introduction to Elliptic Curves and Modular Forms* (Springer-Verlag, 1984).
- [51] S. Antusch and V. Maurer, JHEP **1311** (2013) 115 [arXiv:1306.6879 [hep-ph]].
- [52] F. Björkeröth, F. J. de Anda, I. de Medeiros Varzielas and S. F. King, JHEP **1506** (2015) 141 [arXiv:1503.03306 [hep-ph]].
- [53] M. Tanabashi *et al.* [Particle Data Group], Phys. Rev. D **98** (2018) no.3, 030001.
- [54] NuFIT 4.0 (2018), [www.nu-fit.org/](http://www.nu-fit.org/);  
I. Esteban, M. C. Gonzalez-Garcia, M. Maltoni, I. Martinez-Soler and T. Schwetz, JHEP **1701**, 087 (2017) [arXiv:1611.01514 [hep-ph]].
- [55] Z. Maki, M. Nakagawa and S. Sakata, Prog. Theor. Phys. **28** (1962) 870.
- [56] B. Pontecorvo, Sov. Phys. JETP **26** (1968) 984 [Zh. Eksp. Teor. Fiz. **53** (1967) 1717].
- [57] N. Aghanim *et al.* [Planck Collaboration], arXiv:1807.06209 [astro-ph.CO].
- [58] C. Jarlskog, Phys. Rev. Lett. **55** (1985) 1039.
- [59] P. I. Krastev and S. T. Petcov, Phys. Lett. B **205** (1988) 84.